PHYSICAL REVIEW A VOLUME 57, NUMBER 6 JUNE 1998

Hyperspherical analysis of doubly and triply excited states of Li

Toru Morishita and C. D. Lin
Department of Physics, Kansas State University, Manhattan, Kansas 66506-2601

(Received 7 October 1997)

A computational method for calculating the hyperspherical adiabatic potential curves for three-electron atomic systems is presented. This method allows us to obtain accurate potential curves for any symmetries more efficiently. The potential curves for the Li($^2S^e$) symmetry are analyzed. For the ground state, the energy calculated using the single channel adiabatic approximation is in good agreement with experiment. For doubly excited states, in the region of small and medium hyperradius the potential curves are similar to those for the doubly excited states of two-electron atoms and these curves can be classified using the same set of K, T, and A quantum numbers. For triply excited states, the potential curves are used to show the different Rydberg series that converge to the doubly excited states of Li$^+$. We also illustrate the rotor structure in the energies of triply excited states of Li. [S1050-2947(98)05806-5]

PACS number(s): 31.10.+z, 31.15.Ja, 31.25.Jf

I. INTRODUCTION

In recent years the hyperspherical approach has been extensively used in many areas of few-body systems in physics and chemistry [1–7]. While the mathematical formulation of the hyperspherical method for the general few-body systems has been addressed by many authors [8–10], most of the practical and accurate calculations have been limited to the three-body systems. For the special case of the restricted four-body systems, i.e., the three-electron atomic systems, where one of the particles is very heavy and can be considered fixed in space, early calculations used hyperspherical harmonics as basis functions to expand the wave function of the three electrons [11,12]. While such a method is rigorous in principle, the convergence in general is very slow such that little useful quantitative information can be obtained. To achieve high numerical accuracy and to be able to deal with multiply excited states, more flexible basis functions such as those generated from the Slater-type orbitals [13], the B-spline functions [14,15] and the discrete variable representation (DVR) basis functions [16] have been used. In [14,16], the hyperspherical channel functions have been analyzed for the (s^3) model where the angular correlation among the three electrons is neglected. For the atomic system under study each state has well-defined spin and orbital angular momentum quantum numbers and the parity. Furthermore, the wave function must satisfy the Pauli exclusion principle. To reduce the size of the Hamiltonian matrix, Yang *et al.* [14,15] constructed basis functions from the primitive B-spline functions that have the correct quantum symmetry. However, the calculation of the matrix elements cannot be evaluated accurately and efficiently because the hyperspherical variables are not invariant under particle permutations for the three-electron systems.

In this paper we employ a method of calculating atomic three-electron systems in hyperspherical coordinates. The theoretical method is outlined in Sec. II. We employ the adiabatic approach where the hyperspherical radius is used as an adiabatic parameter. The major steps of the computational method are outlined in Sec. III. The method has been implemented now in a suite of computer codes and potential curves for any symmetries can be calculated. Some results for the H^{2-} system has been reported elsewhere [17] where we showed that no resonances exist for H^{2-}, in contradiction to the recent predictions [18,19]. In Sec. IV we show the calculated hyperspherical potential curves for the $^2S^e$ states of Li. We then identify the curves that support singly excited states, the family of curves that support doubly excited states and triply excited states. The potential curves that support $1s2lnl$ $^2S^e$ doubly excited states are then analyzed. These curves are compared to the $2lnl$ $^{1,3}S^e$ potential curves of He to show the similarities at small and intermediate range of the hyperradius. At large hyperradius, we also show that these curves are described by the independent particle approximation. Proceeding to even higher potential curves we then analyze curves that support triply excited states of Li. The qualitative behavior of these curves will be addressed but the nature of electron correlation of the three electrons in these states remains to be investigated in the future. To illustrate the fact that triply excited states indeed exhibit collective modes as in doubly excited states, we also show potential curves for different symmetries that can be viewed as the rotational excitation of a symmetric top made of the three electrons. These potential curves will be compared to the rotor structure of doubly excited states of Li$^+$. A short summary and future direction are given in Sec. IV to conclude this paper.

II. HYPERSPHERICAL COORDINATES FOR THREE-ELECTRON ATOMS

Starting with the radial distances r_1, r_2, and r_3 of the three electrons from the nucleus, we define the hyperradius R and the two hyperangles α_1 and α_2 as

$$r_1 = R \sin\alpha_2 \cos\alpha_1,$$
$$r_2 = R \sin\alpha_2 \sin\alpha_1, \tag{1}$$
$$r_3 = R \cos\alpha_2.$$

Together with the spherical angles $\hat{\mathbf{r}}_i$ $(i=1,2,3)$ of each electron, the hyperspherical coordinates for the three-electron atoms are $(R,\alpha_1,\alpha_2,\hat{\mathbf{r}}_1,\hat{\mathbf{r}}_2,\hat{\mathbf{r}}_3)$. Thus in the laboratory fixed frame (where the nucleus is stationary), the spatial coordinates of the three electrons are given by the hyperradius R and the eight angles where we shall use $\Omega=\{\alpha_1,\alpha_2,\hat{\mathbf{r}}_1,\hat{\mathbf{r}}_2,\hat{\mathbf{r}}_3\}$ to denote all the angles collectively. The hyperradius is the only coordinate that can extend to infinity. Its magnitude measures the size of the atom. However, at large R, one can have one electron far away while the other two remain close to the nucleus. Examples of such states are singly excited states. One can also have two electrons farther out while the remaining one stays close to the nucleus—these are doubly excited states. Last but not least, one can also have all the three electrons far away from the nucleus. These are examples of triply excited states. Atoms in triply excited states have been called hollow atoms, which have been studied recently using third-generation synchrotron light sources [20,21].

From the theoretical viewpoint, all three types of excited states discussed above are obtainable from the solution of the Schrödinger equation for the three-electron system

$$\left[-\frac{1}{2}\sum_{i=1}^{3}\nabla_i^2+V-E\right]\Psi=0, \tag{2}$$

where V is the Coulomb potential energy due to electron-nucleus and electron-electron interactions. If we rescale the total wave function $\psi=Rr_1r_2r_3\Psi$, then Eq. (2) reads

$$\left[-\frac{1}{2}\frac{\partial^2}{\partial R^2}+H_{\mathrm{ad}}(\Omega;R)-E\right]\psi=0, \tag{3}$$

where the adiabatic Hamiltonian $H_{\mathrm{ad}}(\Omega;R)$ is an operator in Ω which depends parametrically on R, and its explicit form is

$$H_{\mathrm{ad}}(\Omega;R)=-\frac{\tilde{\Lambda}^2(\Omega)}{2R^2}+\frac{C(\Omega)}{R}. \tag{4}$$

Here, $\tilde{\Lambda}^2(\Omega)$ is the square of the rescaled grand angular momentum operator

$$\begin{aligned}\tilde{\Lambda}^2(\Omega)=&-\frac{1}{\sin\,\alpha_2}\frac{\partial}{\partial\alpha_2}\sin\,\alpha_2\frac{\partial}{\partial\alpha_2}-\frac{1}{\sin^2\,\alpha_2}\frac{\partial^2}{\partial\alpha_1^2}\\&+\frac{\mathbf{l}_1^2}{\sin^2\,\alpha_2\,\cos^2\,\alpha_1}+\frac{\mathbf{l}_2^2}{\sin^2\,\alpha_2\,\sin^2\,\alpha_1}+\frac{\mathbf{l}_3^2}{\cos^2\,\alpha_2},\end{aligned} \tag{5}$$

and $C(\Omega)=RV$ is the effective charge

$$C(\Omega)=R\left[-Z\left(\frac{1}{r_1}+\frac{1}{r_2}+\frac{1}{r_3}\right)+\left(\frac{1}{r_{12}}+\frac{1}{r_{23}}+\frac{1}{r_{31}}\right)\right], \tag{6}$$

where Z is the charge of the nucleus.

In the adiabatic picture, the total wave function for the state with total spin S can be written in the form

$$\psi^S=\sum_{\mu}F_{\mu}^{S}(R)\left(\sum_{S_{12}}\Phi_{\mu}^{S,S_{12}}(\Omega;R)\chi_{S_{12}}^{S}\right), \tag{7}$$

where $\Phi_{\mu}^{S,S_{12}}$ is the adiabatic channel function and $\chi_{S_{12}}^{S}=[\{\chi(1)\chi(2)\}^{S_{12}}\chi(3)]^S$ is the total spin function with intermediate spin S_{12}. The adiabatic channel function $\Phi_{\mu}^{S,S_{12}}$ and its associated potential energy $U_{\mu}^{S,S_{12}}(R)$ are defined as solutions of the hyperspherical adiabatic eigenvalue problem

$$[H_{\mathrm{ad}}(\Omega;R)-U_{\mu}(R)]\Phi_{\mu}(\Omega;R)=0. \tag{8}$$

All the functions $\Phi_{\mu}^{S,S_{12}}$ are among solutions to this equation. However, not all the solutions of Eq. (8) satisfy the Pauli exclusion principle. For quartet states, $S=3/2$, the sum over S_{12} in Eq. (7) contains only one term. The spin part is totally symmetric while the spatial component $\Phi_{\mu}^{3/2,1}$, corresponding to a triplet parent, is totally antisymmetric. For doublet states $S=1/2$ there are two spatial components $\Phi_{\mu}^{1/2,0}$ and $\Phi_{\mu}^{1/2,1}$ which multiply singlet and triplet parent spin functions, respectively. These functions form the basis of the two-dimensional representation of the permutation group S_3 and they have degenerate eigenvalues $U_{\mu}^{1/2,0}(R)=U_{\mu}^{1/2,1}(R)$ for all the values of R. Besides the antisymmetric solutions, Eq. (8) also contains totally symmetric solutions that do not satisfy the Pauli exclusion principle and must be omitted.

In Eq. (7), $F_{\mu}^{S}(R)$ is the radial function. Substituting Eq. (7) into Eq. (3) and integrating over the angular functions, a system of coupled differential equations for the radial functions can be obtained. However, the adiabatic approximation allows us to draw much insightful information on the physical system without even solving the hyperradial equation.

III. NUMERICAL PROCEDURE

In order to construct the channel functions satisfying appropriate symmetries, we adopt a two-step numerical procedure that is based on the decomposition of the effective Coulomb charge $C(\Omega)$ into two parts,

$$C(\Omega)=C_{Ze}(\alpha_1,\alpha_2)+C_{ee}(\Omega) \tag{9}$$

with

$$C_{Ze}(\alpha_1,\alpha_2)=-ZR\left(\frac{1}{r_1}+\frac{1}{r_2}+\frac{1}{r_3}\right) \tag{10}$$

and

$$C_{ee}(\Omega)=R\left(\frac{1}{r_{12}}+\frac{1}{r_{23}}+\frac{1}{r_{31}}\right). \tag{11}$$

In the first step we solve the eigenvalue problem for the operator that contains only the nucleus-electron attractive potential,

$$\tilde{H}_{\mathrm{ad}}(\Omega;R)=\frac{\tilde{\Lambda}^2(\Omega)}{2R^2}+\frac{C_{Ze}(\alpha_1,\alpha_2)}{R}. \tag{12}$$

Since the attractive potential $C_{Ze}(\alpha_1,\alpha_2)$ does not depend on the angles $\hat{\mathbf{r}}_i$ $(i=1,2,3)$, the operator $\tilde{H}_{\mathrm{ad}}(\Omega;R)$ commutes with individual angular momenta $\mathbf{l}_i^2$ $(i=1,2,3)$. Thus the eigenfunctions of this operator can be written in the *separable form*

$$\tilde{\Phi}_\nu^\gamma(\Omega;R)=g_\nu^\gamma(\alpha_1,\alpha_2;R)\mathcal{Y}_\gamma^{LM}(\hat{\mathbf{r}}_1,\hat{\mathbf{r}}_2,\hat{\mathbf{r}}_3), \tag{13}$$

where $\gamma=\{l_1l_2l_3l_{12}\}$, and $\mathcal{Y}_\gamma^{LM}(\hat{\mathbf{r}}_1,\hat{\mathbf{r}}_2,\hat{\mathbf{r}}_3)=[\{Y_{l_1}(\hat{\mathbf{r}}_1)Y_{l_2}(\hat{\mathbf{r}}_2)\}^{l_{12}}Y_{l_3}(\hat{\mathbf{r}}_3)]^{LM}$ is the coupled angular momentum of the three electrons. The function $g_\nu^\gamma(\alpha_1,\alpha_2;R)$ satisfies the two-dimensional eigenvalue problem with respect to α_1 and α_2

$$[h_\gamma(\alpha_1,\alpha_2;R)-\tilde{U}_\nu^\gamma(R)]g_\nu^\gamma(\alpha_1,\alpha_2;R)=0, \tag{14}$$

where

$$\begin{aligned}h_\gamma(\alpha_1,\alpha_2;R)&=\langle\mathcal{Y}_\gamma^{LM}|\tilde{H}_{\rm ad}|\mathcal{Y}_\gamma^{LM}\rangle\\&=\frac{1}{2R^2}\left(\frac{1}{\sin\,\alpha_2}\frac{\partial}{\partial\alpha_2}\sin\,\alpha_2\frac{\partial}{\partial\alpha_2}-\frac{1}{\sin^2\,\alpha_2}\frac{\partial^2}{\partial\alpha_1^2}\right.\\&\quad+\frac{l_1(l_1+1)}{\sin^2\,\alpha_2\,\cos^2\,\alpha_1}+\frac{l_2(l_2+1)}{\sin^2\,\alpha_2\,\sin^2\,\alpha_1}\\&\quad\left.+\frac{l_3(l_3+1)}{\cos^2\,\alpha_2}\right)+\frac{C_{Ze}(\alpha_1,\alpha_2)}{R}.\end{aligned} \tag{15}$$

We solve the two-dimensional eigenvalue problem, Eq. (14), numerically using a variational procedure with direct product of discrete variable representation (DVR) basis sets [22].

The functions $\tilde{\Phi}_\nu^\gamma$ form a complete and orthogonal set in the Ω space at each R, and are used as the basis functions in the second step diagonalization to obtain adiabatic potential curves. Since the operator $\tilde{H}_{\rm ad}$ in the first step as well as $H_{\rm ad}$ is invariant under permutation of all three electrons, we can find the functions $\tilde{\Phi}_\nu^{S,S_{12}}$ that also form the basis of the irreducible representation of the S_3 group from linear combinations of the functions $\tilde{\Phi}_\nu^\gamma$, namely,

$$\tilde{\Phi}_{\Gamma\nu}^{S,S_{12}}=\sum_\gamma c_{\Gamma\gamma\nu}^{S,S_{12}}\tilde{\Phi}_\nu^\gamma, \tag{16}$$

where the summation is taken over degenerate states with the same eigenvalue $\tilde{U}_\nu^\Gamma$, i.e., the sum is only over all permutations of the set $l_1l_2l_3$ and the allowed values of l_{12}. Here S and S_{12} are used as indices for the symmetry, Γ is an index that distinguishes antisymmetric functions. To find appropriate coefficients we apply the antisymmetrization operator

$$A=p_E+p_{(123)}+p_{(132)}-p_{(12)}-p_{(23)}-p_{(13)}, \tag{17}$$

namely, for each numerically obtained solution $\tilde{\Phi}_\nu^\gamma$ we calculate the matrix element

$$\langle\tilde{\Phi}_\nu^\gamma\chi_{S_{12}}^S|A|\tilde{\Phi}_\nu^\gamma\chi_{S_{12}}^S\rangle. \tag{18}$$

Because of the separability of the spatial functions, the matrix elements of each component of A can be separated into three parts,

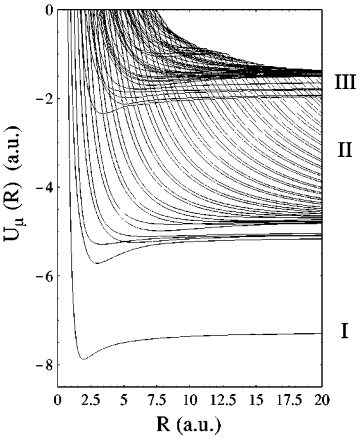

FIG. 1. Hyperspherical potential curves for $^2S^e$ states of Li. The lowest curve labeled I supports the ground state and the $1s^2ns$ singly excited states. The group of potential curves labeled II support doubly excited states $1snln'l'$ while the group of curves labeled III support triply excited states. The lower curves of II and of III are shown in more detail in Fig. 2 and Fig. 3, respectively.

$$\langle\tilde{\Phi}_\nu^\gamma\chi_{S_{12}}^S|p|\tilde{\Phi}_\nu^\gamma\chi_{S_{12}}^S\rangle=\langle g_\gamma^\nu|p|g_\gamma^\nu\rangle\langle\mathcal{Y}_\gamma^{LM}|p|\mathcal{Y}_\gamma^{LM}\rangle\langle\chi_{S_{12}}^S|p|\chi_{S_{12}}^S\rangle. \tag{19}$$

The matrix elements with respect to the spin functions and the spherical harmonics are well known [11,23]. The action of the projection operator on the function $g_\nu^\gamma(\alpha_1,\alpha_2;R)$ is carried out numerically by applying the permutation operators directly on the configuration space defined by the α_1 and α_2 variables. In this manner, we sort out a quartet and two proper components of the doublet basis functions. The potential curves and the channel functions are generated by diagonalizing the matrix

$$\begin{aligned}\langle\tilde{\Phi}_{\Gamma\nu}^{S,S_{12}}|H_{\rm ad}|\tilde{\Phi}_{\Gamma'\nu'}^{S,S_{12}}\rangle&=\tilde{U}_\nu^\Gamma(R)\delta_{\Gamma\Gamma'}\delta_{\nu\nu'}\\&\quad+\frac{1}{R}\langle\tilde{\Phi}_{\Gamma\nu}^{S,S_{12}}|C_{ee}|\tilde{\Phi}_{\Gamma'\nu'}^{S,S_{12}}\rangle\end{aligned} \tag{20}$$

for well-defined total orbital and spin angular momentum quantum numbers and parity.

IV. RESULTS AND DISCUSSION

We have developed the computer codes to calculate the hyperspherical potential curves for any symmetries of the three-electron systems. In the following a subset of such results are shown to illustrate how the properties of a three-electron system are revealed in the hyperspherical approach.

A. The $^2S^e$ states

In Fig. 1 we present the adiabatic potential curves for the $^2S^e$ states of Li. These curves are calculated using $(l_1,l_2,l_3)=(0,0,0)$, (0,1,1), and (1,1,2). There are basically three groups of curves. The first group consists of a single curve—the lowest curve, labeled ''I'' in Fig. 1. This curve supports the ground state and the $1s^2ns$ $^2S^e$ $(n\geqslant 2)$ singly excited Rydberg states. As $R\to\infty$, this curve approaches the $\mathrm{Li}^+(1s^2\ ^1S^e)$ state. The second group, labeled ''II'' in Fig. 1, consists of potential curves that support doubly excited

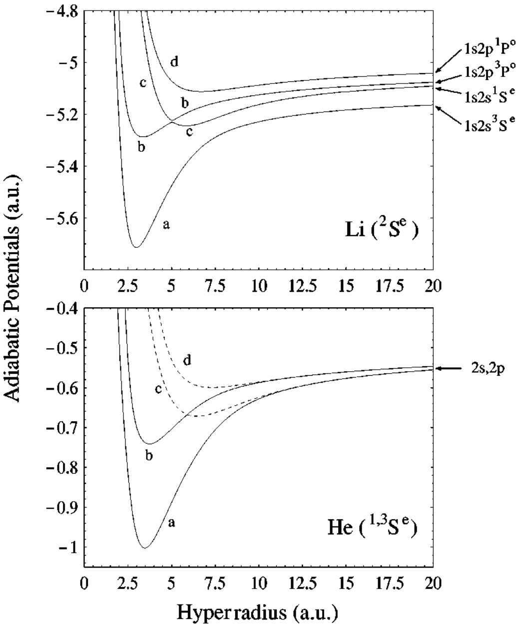

FIG. 2. Comparison of hyperspherical potential curves for $1s2lnl\ {}^2S^e$ doubly excited states of Li with the $2lnl\ {}^{1,3}S^e$ doubly excited states of He. Note that in the inner region the two sets of potential curves are nearly identical. The potential curves for He are designated as $a=(1,0)^+\ {}^1S^e$, $b=(-1,0)^+\ {}^1S^e$, $c=(1,0)^-\ {}^3S^e$, and $d=(-1,0)^-\ {}^3S^e$. These designations can be used for labeling doubly excited states of Li, as indicated. We have assumed that the avoided crossing between b and c in the upper figure can be approximated as a diabatic crossing.

states. These curves approach the $1snl$ ($n\geqslant 2$) singly excited states of Li$^+$ at large R. The third group, labeled ''III,'' consists of potential curves that support triply excited states. These curves approach the $nln'l'$ ($n,n'\geqslant 2$) doubly excited states of Li$^+$ at large R.

1. Ground state and singly excited states

The binding energy of the ground state and singly excited states of Li can be evaluated approximately using the adiabatic approximation. If the second-order diagonal coupling term is included in the potential, the binding energy of the ground state calculated from a single adiabatic channel is -7.466 a.u., which is to be compared to the experimental value of -7.478 a.u. [24]. More accurate results can be obtained if one includes the coupling with the higher channels and basis functions from higher orbital angular momentum components are included. Since the basic properties of ground state and singly excited states of Li are well known from other theoretical approaches, the hyperspherical method just serves as a new method of reproducing known results. Thus no more discussion on this potential curve will be given.

2. Doubly excited states

The second group of potential curves support doubly excited states of Li. To study these states in more detail, we display the lowest four curves of this group in Fig. 2(a). These four curves are to support $1s2sns\ {}^2S^e$ and $1s2pnp\ {}^2S^e$ doubly excited states. There are four Rydberg series and the series limits are $1s2s\ {}^3S^e$, $1s2s\ {}^1S^e$, $1s2p\,{}^3P^o$, and $1s2p\,{}^1P^o$, in increasing order of energy of the Li$^+$ ions. While one may be tempted to assign the resulting Rydberg series associated with these four curves as $1s2s({}^3S^e)ns$, $1s2s({}^1S^e)ns$, $1s2p({}^3P^o)np$, and $1s2p({}^1P^o)np$ series, using the independent particle approximation, we emphasize that such a designation is inappropriate since each adiabatic curve consists of basis functions of all the $(l_1,l_2,l_3)=(0,0,0)$, $(0,1,1)$, and $(1,1,2)$ included in this calculation. From the traditional spectroscopic viewpoint, we expect that the four Rydberg series to have rather strong configuration mixing.

The fact that doubly excited states cannot be described using the independent electron model is well known now. In fact the nature of the four potential curves displayed in Fig. 2 is best understood when compared to the potential curves for the doubly excited states of He. Unlike the doubly excited states of alkali earth atoms, where several analyses have been done by treating a pair of two electrons outside a closed shell core [25–31], here, we study the influence of the $1s$ open shell core on the doubly excited states of three-electron atoms. In Fig. 2(b) we display the hyperspherical potential curves for the ${}^1S^e$ and ${}^3S^e$ states of He that converge to the He$^+$($N=2$) limits. These curves are labeled using the $(K,T)^A$ quantum numbers [1,32–34] as $(1,0)^+\ {}^1S^e$, $(-1,0)^+\ {}^1S^e$ and $(1,0)^-\ {}^3S^e$, and $(-1,0)^-\ {}^3S^e$. By comparing to Fig. 2(a) it is very clear that the two sets of curves are very similar except in the large R region. Thus the potential curves for doubly excited states can be labeled approximately using the quantum numbers used for the doubly excited states of He, at least in the region where the potential curves are near the minima. Watanabe *et al.* [13,35] shows a similar feature of the potential curves for doubly excited states of He$^-$ and of H$^-$. Many properties of the doubly excited states of two-electron atoms can be directly translated to understand the properties of doubly excited states of three-electron atoms—a subject that will be further elaborated on in the future.

The similarities and the differences between the potential curves in Fig. 2(a) and Fig. 2(b) can be understood qualitatively. The lowest state associated with each potential curve is located near the minimum of the potential curve and slightly beyond. Thus the so-called $1s2s^2$ state is associated with the lowest $(1,0)^+\ {}^1S^e$ curve, while the so-called $1s2p^2$ state is associated with the $(-1,0)^+\ {}^1S^e$ curve. For doubly excited states of Li such as $1s2s^2$ and $1s2p^2$, the coupling between the two $n=2$ electrons is larger than the coupling between the $1s$ and $2s$ or $1s$ and $2p$ electrons. Therefore such doubly excited states can be visualized as consisting of one $1s$ electron and a pair of doubly excited electrons. The two excited electrons are classified like the doubly excited states of He since the inner $1s$ electron can almost fully screen the nucleus. In Fig. 2(a) the potential energy contains the energy of the $1s$ electron, which is -4.5 a.u. Removing this difference we can see that the two sets of potential curves are also quite close in magnitude.

The two sets of potential curves do show distinct differences in the large R region. In Fig. 2(a) we drew the curves adiabatically such that in the asymptotic region the curves are labeled as $1s2s({}^3S^e)ns$, $1s2s({}^1S^e)ns$, $1s2p({}^3P^o)np$, and $1s2p({}^1P^o)np$ from below, respectively. Such labelings

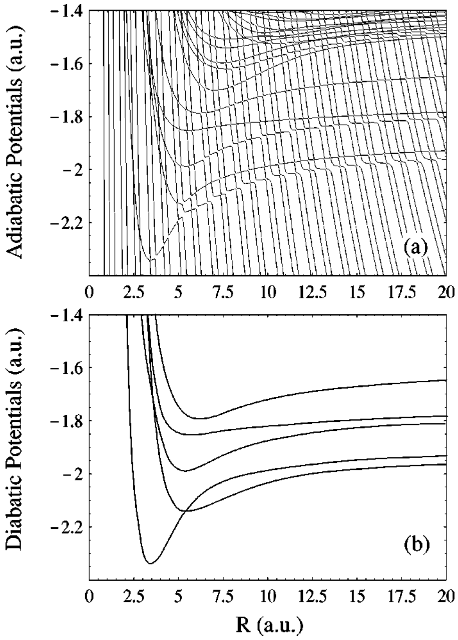

FIG. 3. (a) Potential curves that support triply excited states of Li, shown with numerous avoided crossings with curves that support doubly excited states. (b) The five potential curves that support $2l2l'nl''$ $^2S^e$ triply excited states, with the coupling to doubly excited curves removed.

are good for describing high-lying doubly excited states where $n \gg 2$. In these states the coupling of $1s$ and $2s$ (or $1s$ and $2p$) is much stronger than the coupling of $2s$ with the nl Rydberg electron (or $2p$ and nl). In Fig. 2(a) we drew the potential curves adiabatically such that the $(1,0)^+$ $^1S^e$ curve at small R evolves into $1s2s(^3S^e)ns$ at large R. How valid is such an adiabatic description has to be checked in future numerical calculations with and without including the coupling of these curves. We comment that if the Rydberg series that converges to the $1s2s(^3S^e)$ limit is supported by an adiabatic potential curve as shown in Fig. 2(a), the autoionization width of the series is expected to be rather broad when compared to other series since in the inner region it is clearly a ''+'' series for the two excited electrons. Thus the hyperspherical approach provides a nice way to understand the doubly excited states of Li in terms of the known results of He.

3. Triply excited states

In Fig. 3(a) the first few potential curves that support triply excited states of Li are shown in more detail. These curves display numerous avoided crossings with potential curves that support doubly excited states. The couplings of potential curves are responsible for the autoionization of triply excited states into ground and singly excited states of Li^+ where an autoionized electron will be ejected. To study the general properties of triply excited states we first neglect such couplings. By isolating only triply excited states, we redrew these curves as shown in Fig. 3(b). The five curves shown in Fig. 3(b) support $2l2l'nl''$ triply excited states. Using notations from the independent electron approximation, the five Rydberg series are $2s^2$ $^1S^ens$, $2s2p$ $^3P^onp$, $2p^2$ $^1D^end$, $2s2p$ $^1P^onp$, and $2p^2$ $^1S^ens$. Note that such designation is approximate only since configuration mixing is expected to be rather large. In the future a new set of approximate quantum numbers will be used to label these channels after the nature of correlation among the three electrons is understood.

Among the five curves only the lowest curve has a deep well at small R near 3.0 a.u. This curve supports the only $^2S^e$ intrashell state, which is designated conventionally as $2s2p^2$ $^2S^e$. All the other four $^2S^e$ curves do not have intrashell states. The location of the potential minima of these other curves is shifted further out and the potential well is shallower. Since electron correlation among the three electrons is inherently contained in the multivariable channel functions, full information on each channel will become available only after the wave function is analyzed. The full characterization of triply excited states remains one of the major tasks in the future study of three-electron atomic system.

B. The rotor structure of triply excited states

To study the collective motion of the three electrons in triply excited states, it is natural to examine first the intrashell states. In these states the three electrons are at about the same distances from the nucleus. Like doubly excited states, we then ask if the energies of some triply excited states can be understood as the rotational excitation of a symmetric top formed by the three electrons. Such a question has been addressed previously [23,36] in a model study where the three electrons are restricted to the surface of a sphere with the nucleus at the center. A more restricted model assuming equilateral triangular geometry for the three electrons has been addressed previously by Matveev [37]. To reduce the electronic repulsion, the most favorable geometry would be that the three electrons distribute about an equilateral triangle with the nucleus at the center. However, not all the intrashell states can take such a geometry due to the symmetry constraints on the wave functions imposed by the orbital and spin quantum numbers, the parity and the Pauli exclusion principle. It has been identified that the $n=2$ intrashell $^2P^o$, $^4P^e$, $^2D^e$, and $^2D^o$ states can be understood as the rotational excitation of a symmetric prolate top where the energy levels can be approximated by $E=[L(L+1)-2T^2]/(2I)$ where I is the moment of inertia and T is the projection of L perpendicular to the norm of the plane formed by the three electrons. The T for the four states above are 1, 0, 2, and 1, respectively. In Fig. 4(a) we show the four potential curves for these four states. Indeed the curves look similar to the potential curves for the $(1,0)^+$ rotor series of Li^+ (or He), as shown in Fig. 4(c) where the three intrashell states are $2s^2$ $^1S^e$, $2s2p$ $^3P^o$, and $2p^2$ $^1D^e$ states according to the independent electron notation. Their rotational excitation energy is given by the same formula with $T=0$.

For the other four $n=2$ intrashell triply states it has been shown that their energies are higher due to the existence of a nodal surface in one of the internal coordinates [23,36], in contrast to the four states mentioned in the previous paragraph where the wave functions have no internal nodal surfaces. These four states, $^2S^e$, $^4S^o$, $^2P^e$, and $^2P^o$, are supported by the potential curves shown in Fig. 4(b). Note that these potential curves are not as deep as the curves shown in

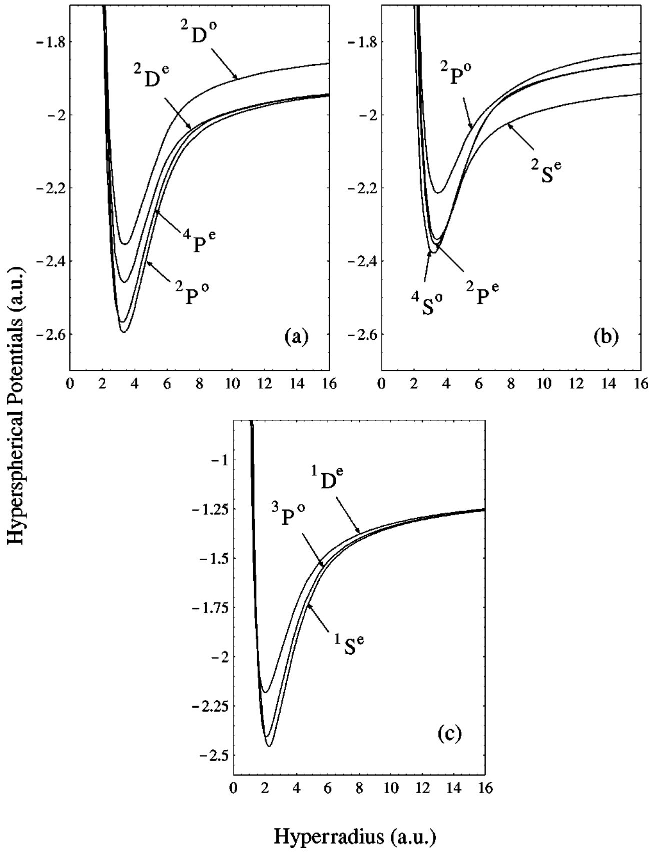

FIG. 4. (a) Potential curves that support intrashell $^2P^o$, $^4P^e$, $^2D^e$, and $^2D^o$ triply excited states. (These states have configurations $2s^22p\ ^2P^o$, $2s2p^2\ ^4P^e$, $2s2p^2\ ^2D^e$, $2p^3\ ^2D^o$ in the independent particle picture.) These states have no nodal surfaces in their internal coordinates and can be understood as the rotational excited states of a symmetric top. (b) The potential curves of the other four intrashell states (called $2p^3\ ^4S^o$, $2s2p^2\ ^2P^e$, $2s2p^2\ ^2S^e$, $2p^3\ ^2P^o$ in the independent particle picture). These states have a nodal surface in one of the internal coordinates; they do not form a rotor series. (c) Potential curves for the three intrashell doubly states of Li^+ in the $n=2$ manifold that form a rotor series.

Fig. 4(a) since the existence of a nodal surface implies higher energies.

We summarize that among the eight intrashell states for the $N=2$ manifold, the $^2P^o$ state is the ground state, the other three states in Fig. 4(a) are due to the rotational excitation, while the other four states in Fig. 4(b) are due to the excitation of one internal nodal surface as well as rotational excitations. This viewpoint deviates from the conventional independent electron model where the eight intrashell states are made out of $2s^22p$, $2s2p^2$, and $2p^3$ configurations. There is no intrinsic contradiction between the two viewpoints, at least for the $N=2$ intrashell states where configuration mixing is not very large in general. The present viewpoint emphasizes the elementary internal normal modes of the system as a whole. This viewpoint can be extended to situations where the independent particle model fails. However, our analysis so far has not accounted for the radial motion of the electrons. When such analysis is available, we would be able to distinguish the nature of all the potential curves for triply excited states.

V. SUMMARY AND CONCLUSIONS

In this paper we present the revised numerical approach for computing the adiabatic hyperspherical potential curves of a three-electron atom. The new method is numerically more accurate and computationally more efficient. Among the results available, in this paper we concentrated on the results for Li ($^2S^e$) states. We show that the ground-state energy can be obtained with reasonable accuracy using just one adiabatic channel. We also show that doubly excited states can be understood and classified similar to the doubly excited states of two-electron atoms, at least in the region near the minimum of each potential curve. This implies that many properties of doubly excited states of Li can be understood based on the doubly excited states of He. We also show the potential curves for the triply excited states. While the separation of different Rydberg series into different potential curves has been achieved, the nature of electron correlation in triply excited states remains to be resolved. For intrashell states, we showed that a subset of them display behavior similar to the rotational excitation of a rigid rotor, while others have higher excitation energies due to the excitation of other internal degrees of freedom.

With the present numerical implementation, the calculation of adiabatic potential curves for three-electron systems no longer posts a big hurdle. However, there remains a great deal of work to be done. On the one hand, it would be desirable to implement the adiabatic expansion of the total wave function to calculate the properties of doubly excited states of Li and He^- such that the spectroscopy of these systems can be understood to the details as in He and H^- [2,4]. This should be possible since the basic physics and the numerical method can be directly carried over from those for the two-electron systems. On the other hand, triply excited states are different. We need to find a method to map the wave functions to extract information of electron correlation in the channel function. This is not straightforward since each channel function has five internal degrees of freedom and we are at most able to visualize two degrees of freedom each time.

ACKNOWLEDGMENT

This work was supported in part by the U.S. Department of Energy, Office of Basic Energy Research, Division of Chemical Sciences.

---

[1] C. D. Lin, Phys. Rep. **257**, 1 (1995), and references therein.
[2] J.-Z. Tang, S. Watanabe, M. Matsuzawa, and C. D. Lin, Phys. Rev. Lett. **69**, 1633 (1992).
[3] O. I. Tolstikhin, S. Watanabe, and M. Matsuzawa, Phys. Rev. Lett. **74**, 3573 (1995).
[4] O. I. Tolstikhin, S. Watanabe, and M. Matsuzawa, J. Phys. B **29**, L389 (1996).
[5] T. Morishita, K. Hino, S. Watanabe, and M. Matsuzawa, Phys. Rev. A **53**, 2345 (1996).
[6] A. Ohsaki and H. Nakamura, Phys. Rep. **187**, 1 (1990).

[7] J. M. Launay and M. le Dourneuf, Chem. Phys. Lett. **169**, 473 (1990).

[8] M. Cavagnero, Phys. Rev. A **30**, 1169 (1984); **33**, 2877 (1986); **36**, 523 (1987).

[9] A. Novoselsky and N. Barnea, Phys. Rev. A **51**, 2777 (1995).

[10] U. Fano and A. R. P. Rau, *Symmetries in Quantum Physics* (Academic Press, San Diego, 1996), Chap. 10.

[11] C. W. Clark and C. H. Greene, Phys. Rev. A **21**, 1786 (1980).

[12] C. H. Greene and C. W. Clark, Phys. Rev. A **30**, 2161 (1984).

[13] S. Watanabe, M. Le Dourneuf, and L. Pelamourgues, J. Phys. (Paris), Colloq. **43**, C2-223 (1982); S. Watanabe, in *Multiphoton Processes,* Cambridge Studies in Modern Optics Vol. 8, edited by S. J. Smith and P. L. Knight (Cambridge University Press, Cambridge, 1988), pp. 292–303.

[14] X. Yang, J. Xi, C. G. Bao, and C. D. Lin, Phys. Rev. A **52**, 2029 (1995).

[15] X. Yang, C. G. Bao, and C. D. Lin, Phys. Rev. A **53**, 3934 (1996).

[16] T. Morishita, O. I. Tolstikhin, S. Watanabe, and M. Matsuzawa, Phys. Rev. A **56**, 3559 (1997).

[17] T. Morishita, C. D. Lin, and C. G. Bao, Phys. Rev. Lett. **80**, 464 (1998).

[18] T. Sommerfeld, U. V. Riss, H.-D. Meyer, and L. S. Cederbaum, Phys. Rev. Lett. **77**, 470 (1996).

[19] T. Sommerfeld, U. V. Riss, H.-D. Meyer, and L. S. Cederbaum, Phys. Rev. A **55**, 1903 (1997).

[20] T. Azuma, S. Hasegawa, F. Koike, G. Kutluk, T. Nagata, E. Shigemasa, A. Yagishita, and I. A. Sellin, Phys. Rev. Lett. **74**, 3768 (1995); T. Azuma, F. Koike, J. W. Cooper, T. Nagata, G. Kutluk, E. Shigemasa, R. Wehlitz, and I. A. Sellin, *ibid.* **79**, 2419 (1997).

[21] L. Journel *et al.*, Phys. Rev. Lett. **76**, 30 (1996); S. Diehl *et al.*, *ibid.* **76**, 3915 (1996); D. Cubaynes *et al.*, *ibid.* **77**, 2194 (1996); S. Diehl *et al.*, Phys. Rev. A **56**, R1071 (1997); S. Diehl *et al.*, J. Phys. B **30**, L595 (1997).

[22] D. O. Harris, G. G. Engerholm, and W. D. Gwinn, J. Chem. Phys. **43**, 1515 (1965); A. S. Dickinson and P. R. Certain, *ibid.* **49**, 4209 (1968); J. C. Light and R. B. Walker, *ibid.* **65**, 4272 (1976); J. C. Light, I. P. Hamilton, and J. V. Lill, *ibid.* **82**, 1400 (1985).

[23] S. Watanabe and C. D. Lin, Phys. Rev. A **36**, 511 (1987).

[24] D. K. McKenzie and G. W. F. Drake, Phys. Rev. A **44**, 6973 (1991).

[25] C. H. Greene, Phys. Rev. A **23**, 661 (1981).

[26] P. F. O'Mahony and C. H. Greene, Phys. Rev. A **31**, 250 (1985).

[27] P. F. O'Mahony and S. Watanabe, J. Phys. B **18**, L239 (1985).

[28] M. E. Kellman, Phys. Rev. Lett. **55**, 1738 (1985).

[29] R. S. Berry and J. L. Krause, Phys. Rev. A **33**, 2865 (1986).

[30] B. Zhou and C. D. Lin, Phys. Rev. A **51**, 1286 (1995).

[31] S. Watanabe and T. Ebara, Phys. Rev. A **55**, 175 (1997).

[32] D. R. Herrick and O. Sinanoĝlu, Phys. Rev. A **11**, 97 (1975).

[33] M. E. Kellman and D. R. Herrick, J. Phys. B **11**, L755 (1978).

[34] M. E. Kellman and D. R. Herrick, Phys. Rev. A **22**, 1536 (1980).

[35] M. Le Dournouf and S. Watanabe, J. Phys. B. **23**, 3205 (1990).

[36] C. G. Bao, X. Z. Yang, and C. D. Lin, Phys. Rev. A **55**, 4168 (1997).

[37] V. I. Matveev, Zh. Éksp. Teor. Fiz. **89**, 411 (1985) [Sov. Phys. JETP **62**, 233 (1985)].